Laser and Particle Beams (2000), *18*, 595–600. Printed in the USA.

Diagnosis of peak laser intensity from high-energy ion measurements during intense laser interactions with underdense plasmas

K. KRUSHELNICK,[1] E. CLARK,[1,4] Z. NAJMUDIN,[1] M. SALVATI,[1] M.I.K. SANTALA,[1] M. TATARAKIS,[1] A.E. DANGOR,[1] V. MALKA,[2] D. NEELY,[3] R. ALLOTT,[3] AND C. DANSON[3]

[1]Imperial College of Science, Technology & Medicine, Prince Consort Road, London, SW7 2BZ, U.K.
[2]Laboratoire pour l'Utilisation des Lasers Intenses (LULI) Unité mixte no. 7605 CNRS—CEA—École Polytechnique—Université Pierre et Marie Curie, France
[3]Rutherford Appleton Laboratory, Chilton, Didcot , Oxon., U.K.
[4]Radiation Physics Department, AWE plc, Aldermaston, Reading RG7 4PR, U.K.

(RECEIVED 9 August 1999; ACCEPTED 13 June 2000)

Abstract

Experiments were performed using high-power laser pulses (greater than 50 TW) focused into underdense helium, neon, or deuterium plasmas ($n_e \leq 5 \times 10^{19}$ cm^{-3}). Ions having energies greater than 300 keV were measured to be produced primarily at 90° to the axis of laser propagation. Ion energies greater than 6 MeV were recorded from interactions with neon. Spatially resolved pinhole images of the ion emission were also obtained and were used to estimate the intensity of the focused radiation in the interaction region.

1. INTRODUCTION

Over the past several years, there have been rapid advances in the use of high-power, short-pulse lasers (Perry & Mourou, 1994). In particular, the potential of such lasers for applications in particle acceleration (Tajima & Dawson, 1979; Sprangle *et al.*, 1988; Esarey *et al.*, 1996), X-ray generation, and inertial confinement fusion (Tabak *et al.*, 1994) seems promising. However, much of the highly nonlinear plasma physics that occurs during such interactions is not well understood and experiments that address the fundamental physics of these interactions are required to properly evaluate the suitability of these intense laser-produced plasmas for such applications. Because of the complexity of interactions at ultra-high intensity and the short temporal and spatial scales, direct observations of the properties of the laser-produced plasma as well as measurements of the laser pulse itself during the interaction are difficult.

In this article, we discuss details of recent measurements (Krushelnick *et al.*, 1999) of accelerated ions produced by the "Coulomb explosion" of a high-intensity laser-produced plasma (Burnett & Enright, 1990). In our experiments, ions are accelerated by electrostatic forces caused by charge separation induced by the laser ponderomotive pressure. We find that a spatially resolved measurement of the high-energy ions can provide a direct and simple estimate of the laser intensity in the plasma. By imaging ion emission, it may be possible to estimate how the intensity of the laser pulse changes as it propagates through the underdense plasma. In these experiments, we have measured peak ion energies of 1.0 MeV for deuterium gas interactions, 3.6 MeV for helium interactions and greater than 6 MeV for interactions with neon.

Such measurements indicate that the peak laser intensity achieved during these experiments was greater than $\sim 6 \times 10^{19}$ W/cm^2. This provides evidence that, in our experiments, significant relativistic/charge-displacement self-focusing of the laser pulse occurs as it propagates through the plasma (of greater than a factor of 7). Previous computer modeling of such interactions has inferred that intense laser pulses can be self-focused to such intensities (Pukhov & Meyer-ter-Vehn, 1997); however, the further use of the techniques discussed here may lead to direct diagnosis of the laser intensity during such interactions. Previous measurements of MeV ion emission have been obtained from laser plasma interactions at high density ($n_e \sim n_{crit}$) (Gitomer *et al.*, 1986; Fews *et al.*, 1994) where the ions are accelerated in the ablated plasma due to space-charge forces generated by escaping hot electrons. Earlier experiments using under-

Address correspondence and reprint requests to: Karl Krushelnick, Imperial College, Department of Physics, Blackett Laboratory, SW7 2BZ, London, U.K. E-mail: kmkr@ic.ac.uk

dense plasmas were performed at much lower intensities and have measured ions accelerated by the laser ponderomotive force up to energies of 50 keV (Young *et al.*, 1996).

The production of energetic ions has also been inferred previously from observations of a plasma channel left trailing the high intensity laser pulse as it propagates through the underdense plasma (Krushelnick *et al.*, 1997; Chen *et al.*, 1998; Sarkisov *et al.*, 1999). The generation of this channel is due to the expansion of energetic ions via the momentum given to them during a Coulomb explosion (see Fig. 1). As a very high intensity laser pulse propagates through an underdense plasma, the strong ponderomotive force of the laser pulse forces some of the electrons from the region of highest intensity. Ions are affected much less by the ponderomotive force due to their larger mass. However, as the laser pulse passes, these ions will be given an impulse perpendicular to the laser axis, which is produced by the large space-charge forces caused by charge separation. After the laser pulse passes, electrons will return to their original positions on a timescale of about $1/\omega_{pe}$, (where ω_{pe} is the plasma frequency); however, the transverse momentum given to the ions will be retained and they will continue moving out of the plasma, carrying low-energy electrons with them. The energy of these ions is thus directly related to the intensity of the focused laser pulse, and the maximum energy that can be gained by an ion during these interactions is simply given as the relativistic ponderomotive energy ($U = Zm_e c^2(\gamma - 1)$ where Z is the ion charge and γ is the relativistic factor of the electron quiver motion in the laser field).

2. EXPERIMENTAL PROCEDURE

Our experiments were performed using the VULCAN laser at Rutherford Appleton Laboratory. This system produces laser pulses having an energy of up to 50 J , and a duration of 0.9 ps at a wavelength of 1.054 μm (Nd:Glass). The laser pulse was focused into a gas jet target (4 mm nozzle diameter) using an f/4 off-axis parabolic mirror. When helium was used as the target gas, the plasma had an electron density up to about 5×10^{19} cm^{-3}. The plasma electron density during the interaction was determined by the wavelength shift of laser light scattered by the forward Raman scattering instability. Deuterium and neon were also used as target gases.

In our experiments, the angular distribution of ions emitted during such high-intensity laser plasma interactions was recorded using CR-39 nuclear track detectors placed at various positions surrounding the interaction region and which are sensitive to helium ions greater than about 300 keV (Fews, 1992*a*, 1992*b*) (see experimental setup in Fig. 2). As an energetic ion collides with the detector, it causes structural damage in the material so that an observable track can be recorded for each ion. In this way, the total number of ions can be counted. It was found that there was no significant variation in ion emission in the azimuthal direction (i.e., changing the laser polarization had little effect). However, a distinct peak was observed in the emission of ions with energies greater than 300 keV at 90° to the axis of propagation. Measurements of the ion emission at higher energies were also obtained by using CR-39 track detectors covered with thin

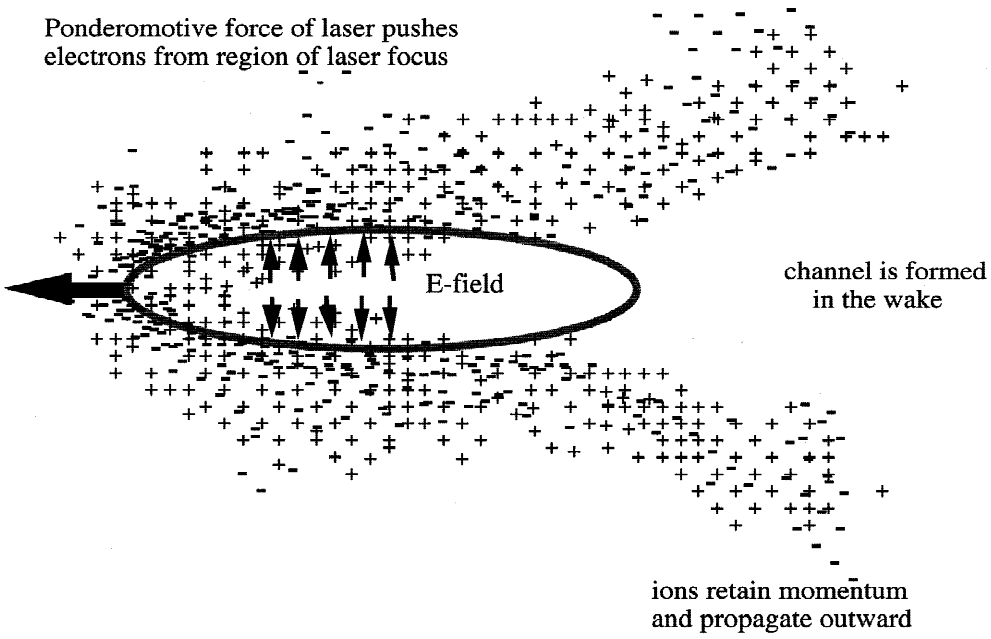

Fig. 1. Schematic of "Coloumb Explosion."

https://doi.org/10.1017/S0263034600184034 Published online by Cambridge University Press

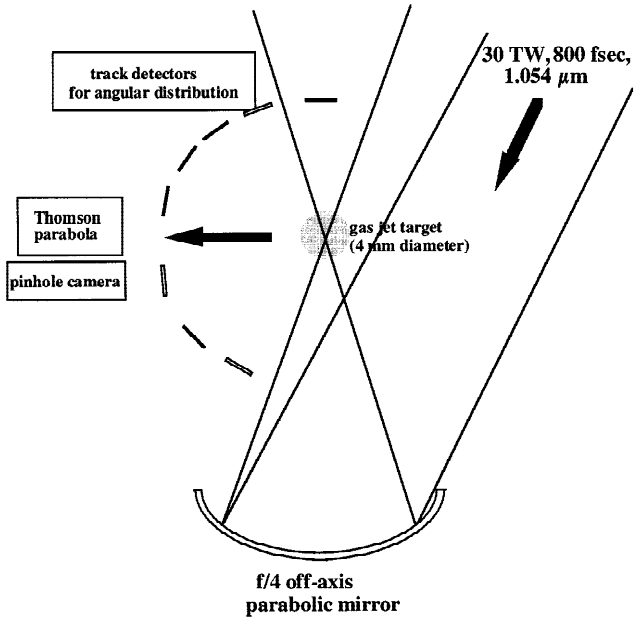

Fig. 2. Experimental setup.

aluminum filters (2 μm) that will block all signal from helium ions below about 2 MeV in energy.

3. RESULTS AND DISCUSSION

Averaged measurements over four shots are shown in Figure 3. It is clear that the majority of ion emission occurs in the 90° direction, although the emission lobe also extends in the backward direction somewhat. Emission at energies greater than 2 MeV shows a narrower lobe in the 90° direction. Simultaneous measurements over a wide range of angles (i.e., lower resolution measurements) indicated that there was some spatial structure in the ion emission pattern, which seemingly corresponds to bursts of ions emitted at certain narrow angles and which changes from shot to shot.

The ion energy spectrum can be calculated by simply balancing the force due to charge separation ($\nabla \cdot \boldsymbol{E} = -4\pi e \delta n_e$) with the ponderomotive force of the laser on the electrons [$\boldsymbol{F} = -mc^2 \nabla (1 + a^2/2)^{1/2}$, where a is the normalized vector potential of the laser pulse, $a = (eE_L)/m\omega_L c$]. The momentum imparted to an ion by the resulting space-charge force acting over the duration of the laser pulse is then calculated. Such calculations indicate that the maximum ion energy is directly dependent on the intensity of the focused laser pulse, and that this energy is well defined. An experimentally obtained ion spectrum will be the result of interactions over a wide range of laser intensities—however the peak ion energy observed in the spectrum should correspond approximately to the maximum laser intensity in the plasma. In these experiments, the laser intensity was unlikely to be sufficiently large to force all of the plasma electrons from the focal region (cavitation), so it may be possible to use this simple theoretical model for interpretation of our experiments. Large amounts of stimulated Raman side-scatter were also observed in these experiments, which is theoretically expected to suppress cavitation (Tzeng & Mori, 1998).

The spectrum of the energetic ions was measured using a Thomson parabola that spatially separates ion species having different charge-to-mass ratios through the use of parallel electric and magnetic fields. CR-39 was used as the detector. The spectrometer was positioned at 42 cm from the laser interaction at 90° from the axis of propagation and used a 250-μm diameter pinhole as the aperture. Typical experimentally measured spectra are shown in Figure 4 for neon, which extends to energies greater than 6 MeV. The spectra in Figure 4 also show good qualitative agreement with a recently published ion spectra from PIC calculations ($I = 2 \times 10^{18}$ W/cm^2) (Pretzler *et al.*, 1998).

For helium interactions, it is estimated that 0.25% of the incident laser energy is transferred to ions having greater than 300 keV of energy by using the previously measured ion angular emission profiles. It is interesting to note that, in helium plasmas, both He^{1+} and He^{2+} ions were observed with very high energy. In the interaction region, helium ions are completely ionized since the intensity required to directly field ionize He^{1+} is about 10^{16} W/cm^2. This implies that the He^{1+} is generated by charge-exchange/recombination of ions as they travel out of the gas jet to the detector. The classical charge-exchange cross section is given approximately by $\sigma \cong (\pi (Z_1 Z_2 e^2)^2)/\Delta E^3$ (where Z_1 and Z_2 are the charge states of the two species and ΔE is the difference in kinetic energy) (Mapleton, 1972). This indicates that lower energy ions will have a significantly enhanced probability of charge exchange with the neutral atoms in the surrounding gas, agreeing with our observations of the ion spectra that higher ionization states had a higher peak energy. Note that the charge-exchange process does not affect the ion energies significantly. In neon interactions, the atoms can be stripped up to the Ne^{8+} stage from direct field ionization; however only neon species up to Ne^{5+} were observed in our experiment, also indicating significant charge exchange/recombination.

The process of relativistic/charge-displacement self-focusing is not exactly reproducible from shot to shot, because it is sensitive to small changes in density gradients in the gas jet as well as fluctuations in the initial beam profile of the incident laser. The maximum ion energy, such that there were more than 10^8 ions/MeV/sterradian, was found to be 3.6 MeV for helium, 1.0 MeV for deuterium, and greater than 6 MeV for neon. In Figure 5 we present a plot of peak ion energy *versus* laser energy, where the large variation in peak ion energy should be noted. It is possible to use these measured energies as a diagnostic of the peak laser intensity during the laser plasma interaction. These interactions are well above the critical power threshold for relativistic self-focusing ($P_{crit} = 17\ (n_{crit}/n_e)$ GW $= 1.7$ TW for plasmas of densities 10^{19} cm^{-3}) so that it is expected that there will be a significant enhancement of the peak laser intensity during the interaction. This is precisely what is observed if we cal-

https://doi.org/10.1017/S0263034600184034 Published online by Cambridge University Press

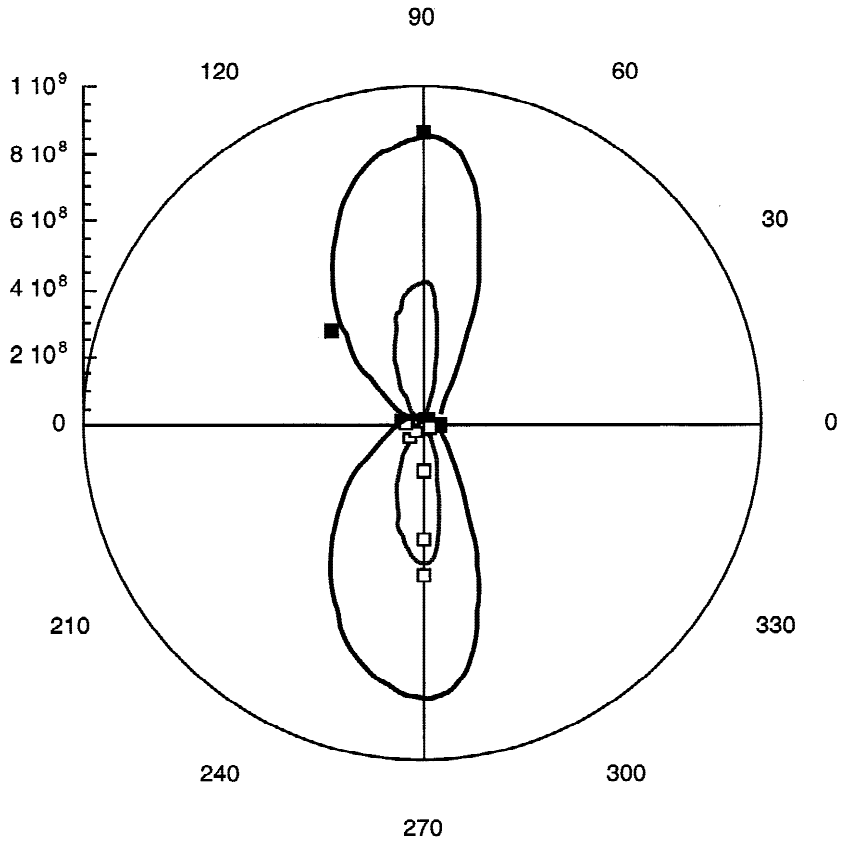

Fig. 3. Angular emission of energetic ions. Dark line: distribution of helium ions with energy greater than 400 keV. Light line: distribution of helium ions with energy greater than 2 MeV (shown × 10). (Note that lines are drawn as a visual aid only.)

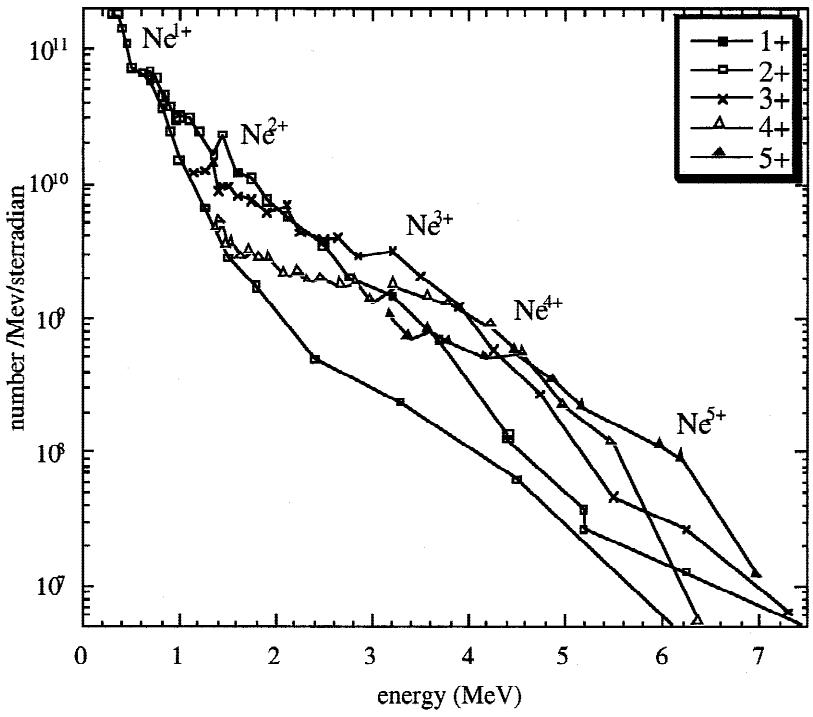

Fig. 4. Typical ion spectrum from neon interaction (90°).

https://doi.org/10.1017/S0263034600184034 Published online by Cambridge University Press

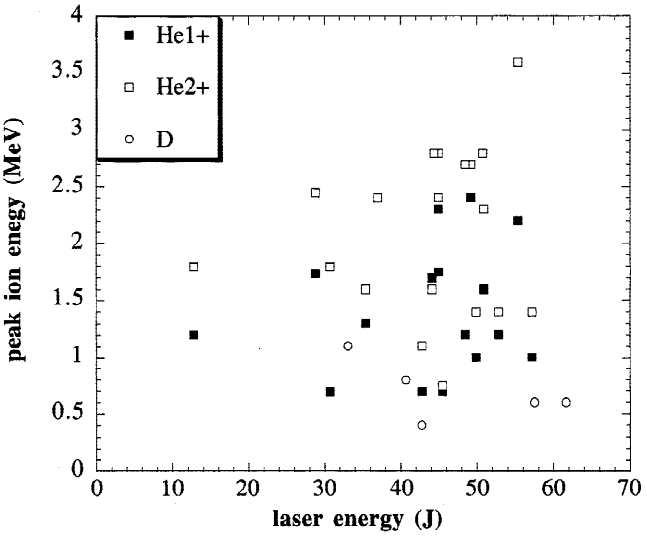

Fig. 5. Variation of peak ion energy with laser pulse energy.

culate the necessary laser intensity to produce the observed ion spectra. In Figure 6, a plot of the estimated peak laser intensity in the plasma (obtained from the peak ion energy) *versus* the "expected" laser intensity from the measured laser parameters (pulse length, energy, far-field focal spot) is presented. It is clear that the effect of the plasma is typically to increase the laser intensity in the interaction region. All of the data from our measurements are presented here and it should be noted that there is a significant shot-to-shot variation in these results, probably due to the nonlinear nature of the self-focusing processes. However, it should be stressed that accurate diagnosis of the interaction will require comparison to sophisticated computer simulations. The estimates of the laser intensity during the interactions with neon gas (less than the "vacuum" intensity) suggest that the effects of ionization-induced diffraction can also counteract any self-focusing processes and cause the intensity to be reduced during such interactions.

Ion emission was also spatially resolved using pinhole imaging. A large diameter pinhole (250-μm diameter) was used for measurement of the ion images onto CR-39. The magnification used ($\sim$ 2:1) was such that it was possible to obtain a rough image of the regions of most intense ion emission from the laser-produced plasma. Images were obtained for helium and deuterium gas interactions. An example ion image of a helium interaction having multiple focuses is shown in Figure 7. Because there was typically a significant number of energetic neutrals, it was also possible to create an image of the interaction region using the neutral particles and then to add a magnetic field to determine the maximum ion energy. In this way it may be possible to determine the peak laser intensity throughout the interaction region. Multiple focal spots in the ion images were also found to be correlated with optical images of the Thomson scattered light during these interactions. We also obtained ion images using a charge-coupled device (CCD) array as the detector for the energetic ions, which shows qualitatively similar structure to that obtained with optical diagnostics (see Fig. 8). The spatial structure shown in Figures 7 and 8 may also provide evidence of filamentation effects occurring as the intense laser pulse propagates through the plasma.

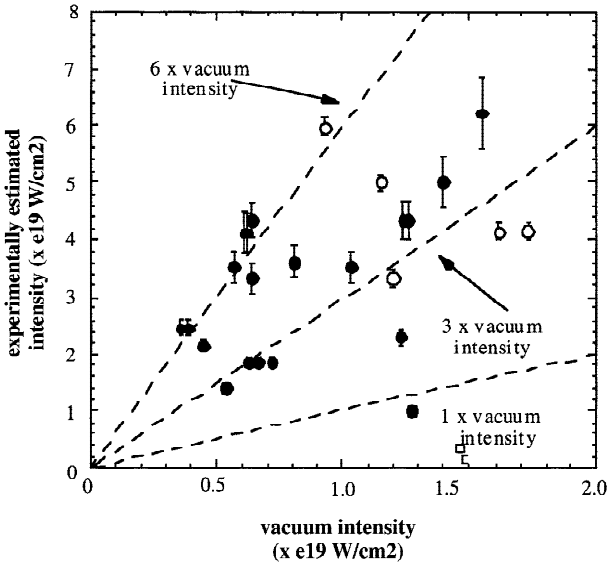

Fig. 6. Experimentally estimated laser intensity in plasma (from peak ion energy) *versus* expected "vacuum" intensity (from simultaneous measurements of laser parameters). Black circles: helium; white circles: deuterium; squares: neon. Dashed lines are drawn as a visual aid only.

4. CONCLUSION

These experiments have shown that energetic ions are produced primarily in the 90° direction during these interactions and that the generation mechanism can be understood as a result of Coulomb explosion processes. We have shown that neon ions greater than 6 MeV and helium ions up to

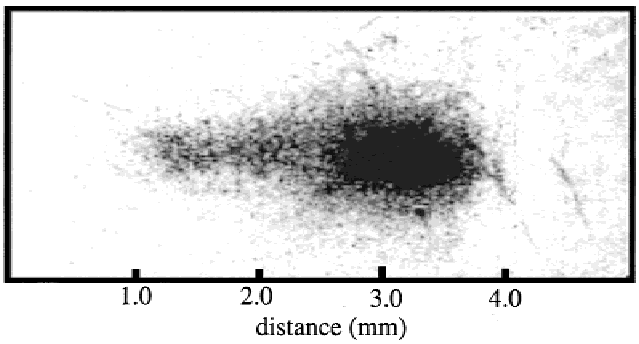

Fig. 7. Pinhole ion image of typical helium interaction recorded on CR-39. Laser propagates from right to left.

https://doi.org/10.1017/S0263034600184034 Published online by Cambridge University Press

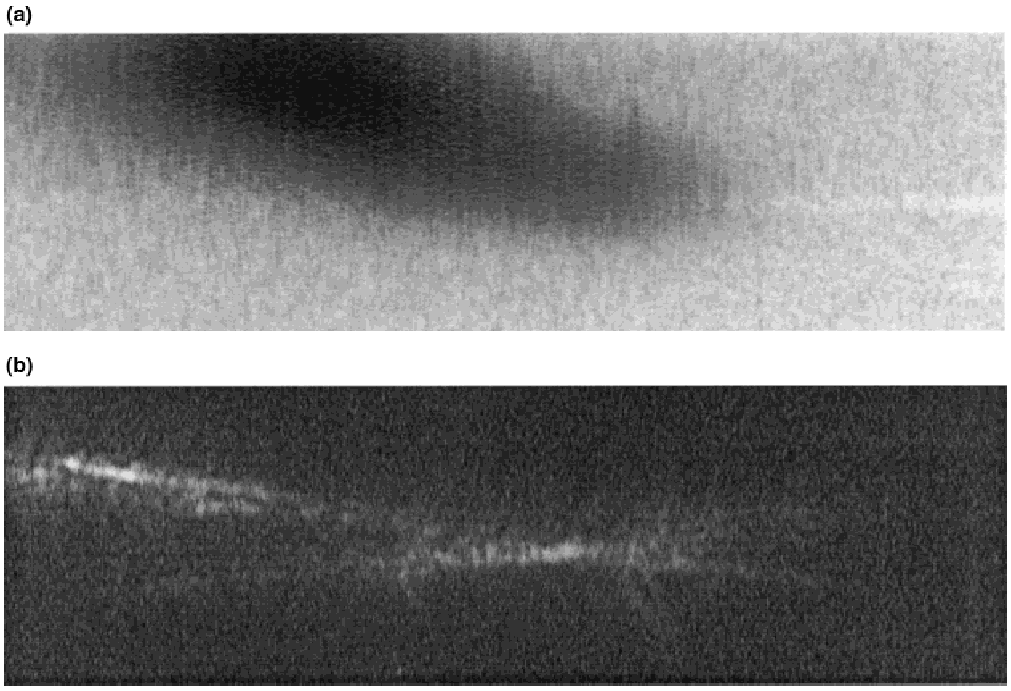

Fig. 8. (a) CCD image of ion emission. (b) Second harmonic emission from plasma during interaction (note qualitatively similar structure).

4 MeV can be generated. From these measurements it is likely that, during our experiments, the laser pulse undergoes significant self-focussing as a result of relativistic and charge-displacement effects throughout the interaction region.

These results are important because they may lead to the use of a new and potentially powerful diagnostic for direct measurement of the intensity of very high power laser pulses inside an underdense plasma. At much higher densities, energetic ions created by such processes may carry a significant amount of the incident laser energy, and the transfer of energy into ions may therefore be important when considering the use of such laser pulses as a "Fast Ignitor" in inertial confinement fusion experiments (Tabak *et al.*, 1994). This phenomenon may also be useful as a point source of energetic neutrons, if high repetition rate laser interactions with a deuterium–tritium gas jet can induce a significant number of thermonuclear fusion reactions between laser-accelerated ions and those in the surrounding gas (Goloviznin & Schep, 1998).

ACKNOWLEDGMENTS

The authors would like to acknowledge useful discussions with A.P. Fews and P. Norreys as well as technical assistance from the VULCAN operations team.

REFERENCES

Burnett, N.H. & Enright, G.D. (1990). *IEEE J. Quant. Electron.* **26**, 1797.
Chen, S.Y. *et al.* (1998). *Phys. Rev. Lett.* **80**, 2610.
Coverdale, C. *et al.* (1995). *Phys. Rev. Lett.* **74**, 4659.
Esarey, E. *et al.* (1996). *IEEE Trans. Plasma Sci.* **24**, 252.
Fews, A.P. (1992*a*). *Nucl. Instrum. Methods Phys. Res. B* **71**, 465.
Fews, A.P. (1992*b*). *Nucl. Instrum. Methods Phys. Res. B* **72**, 91.
Fews, A.P. *et al.* (1994). *Phys. Rev. Lett.* **73**, 1801.
Gitomer, S.J. *et al.* (1986). *Phys. Fluids* **29**, 2679.
Goloviznin, V.V. & Schep, T.J. (1998). *J. Phys. D* **31**, 3243.
Krushelnick, K. *et al.* (1997). *Phys. Rev. Lett.* **78**, 4047.
Krushelnick, K. *et al.* (1999). *Phys. Rev. Lett.* **83**, 737.
Mapleton, R.A. (1972). *The Theory of Charge Exchange*. New York: Wiley-Interscience.
Modena, A. *et al.* (1995). *Nature* **377**, 606.
Nakajima, K. *et al.* (1995). *Phys. Rev. Lett.* **74**, 4428.
Perry, M. & Mourou, G. (1994). *Science* **264**, 917.
Pretzler, G. *et al.* (1998). *Phys. Rev. E* **58**, 1165.
Pukhov, A. & Meyer-Ter-Vehn, J. (1997). *Phys. Rev. Lett.* **79**, 2686.
Sarkisov, G.S. *et al.* (1999). *Phys. Rev. E* **59**, 7042.
Sprangle, P. *et al.* (1988). *Appl. Phys. Lett.* **53**, 2146.
Tabak, M. *et al.* (1994). *Phys. Plasmas* **1**, 1626.
Tajima, T. & Dawson, J.M. (1979). *Phys. Rev. Lett.* **43**, 267.
Ting, A. *et al.* (1997). *Phys. Plasmas* **4**,1889.
Tzeng, K.C. & Mori, W.B. (1998). *Phys. Rev. Lett.* **81**, 104.
Umstadter, D. *et al.* (1996). *Science* **273**, 472.
Young, P.E. *et al.* (1996). *Phys. Rev. Lett.* **76**, 3128.